PAPER 49 (SESSION V)

The effect of temperature on fatigue fracture in a directionally-solidified nickel-base superalloy

M. GELL and G. R. LEVERANT

Advanced Materials Research and Development Laboratory, Pratt & Whitney Aircraft, Middletown, Connecticut, U.S.A.

Summary

A study was made of the fatigue deformation and fracture of the nickel-base superalloy, MAR-M200, in single crystal and columnar-grained forms at 1400°F (760°C) and 1700°F (927°C), and the results were compared with those previously obtained at room temperature. It was found that at room temperature and at low cyclic strains at 1400°F, most cracking was in the Stage I mode (on {111} slip planes); whereas, at 1700°F, cracking was generally in the Stage II mode (non-crystallographic). At high strains at 1400 °F, both Stage I and Stage II cracking occurred. All deformation at room temperature was concentrated in coarse, planar bands; whereas, as the temperature was increased to 1700° F, the deformation became more homogeneous. It is shown that the change in the mode of crack propagation with temperature is related to the corresponding change in deformation mode. It is concluded that Stage I cracking is favored under conditions of planar slip and Stage II cracking under conditions of wavy or more homogeneous slip.

At low strain ranges at all temperatures, a single crack propagated to failure. The initiation site for this crack shifted from the surface to the specimen interior with increasing temperature. These observations are used to show that elevated temperature oxidation retards crack growth.

Introduction

The terms 'Stage I' and 'Stage II', introduced by Forsyth [1], are now commonly used to describe the two different modes of fatigue crack propagation that occur in most pure metals and alloys. Cracking in the Stage I mode occurs on crystallographic slip planes and involves partially reversible dislocation motion in slip bands coplanar with the crack [2-7]. Stage II cracking is non-crystallographic and occurs on surfaces approximately normal to the stress axis. The plastic blunting model proposed by Laird [5], which is appropriate for describing Stage II fracture in many materials, requires extensive irreversible plastic deformation at the crack tip.

Recently, Wells [8] has suggested that the mode of fatigue cracking is related to the slip character [9] of a material. Stage I cracking is favored in materials which deform by planar slip (cross slip of screw dislocations is difficult) and Stage II cracking in materials which deform by wavy slip (cross slip is easy). It is thought by the present authors that the conditions for extensive irreversible deformation at the crack tip needed for Stage II propagation can also be satisfied by closely-spaced

multiple slip, or dislocation climb at elevated temperatures. To evaluate these concepts, this study relates the change in mode of fatigue cracking of a nickel-base superalloy with temperature to the accompanying deformation modes. Deformation in a localized area will be considered to occur by *planar slip* if it is on a single plane or closely-spaced parallel planes or by *homogeneous slip* if it is on closely-spaced intersecting planes or involves profuse cross slip or dislocation climb. As part of the above work, the characteristics of elevated temperature fatigue cracking and the effect of temperature on crack initiation have been determined and will also be discussed.

Experimental procedure

The material used in this study was the nickel-base superalloy, MAR-M200, directionally-solidified into columnar-grained and single crystal forms. The nominal composition in weight per cent was 0·15C, 9Cr, 12·5W, 10Co, 5Al, 2Ti, 1Cb, 0·05Zr, 0·015B, bal. Ni. The material was solutionized for one to four hours at 2250 °F followed by aging at 1600 °F for 32 hours, which resulted in 0·2% offset yield stresses of 150,000 psi at room temperature, 144,000 psi at 1400 °F and 95,000 psi at 1700 °F.

Specimen design, testing procedures and alloy microstructure have all been described previously [7, 10, 11] and will only be summarized here. Following the aging treatment, MAR-M200 contains a cuboidal, γ' precipitate ($Ni_3[Al,Ti]$), 0·3μ on edge, which is ordered and coherent with the γ matrix. After testing at 1700 °F, the precipitate is slightly enlarged and its corners are rounded. The alloy also contains a small volume fraction of micropores, and MC carbides, some of which contain pre-existing cracks [7].

Axial fatigue tests were conducted in air over a wide range of strain amplitudes in the high- and low-cycle fatigue regions, with specimen lives varying from about 10^2 to 10^7 cycles. Low-cycle fatigue tests were strain-controlled with strain varied between zero and a maximum tensile value at a frequency of about 2 cycles per minute. High-cycle fatigue tests were stress-controlled with the stress varied between 5,000 psi and a maximum tensile value less than the yield stress at a frequency of 10 cycles per second. The temperature in the gage section was controlled to ±2 °F. The specimen axis was within five degrees of the [001] growth axis of the single crystals and the common [001] axis of the columnar-grained material. Specimen gage sections were electropolished prior to testing.

Experimental results

A. Comparison of single crystal and columnar-grained materials

In a number of the columnar-grained specimens tested at both 1400 and 1700 °F, crack initiation occurred at MC-type carbides and micropores

located on transverse grain boundary segments. There were also infrequent observations of intergranular propagation. In spite of these grain boundary effects, the location of the initiation sites (surface or interior), the predominant mode of crack propagation, and the fatigue lives of the single crystal and columnar-grained materials were all the same. Because the grain boundary effects were small, they will not be mentioned further in this report.

B. Crack initiation and propagation at 1700 °F (927 °C)

In specimens cycled at low total strain ranges ($0{\cdot}003 \leq \Delta\epsilon_T \leq 0{;}006$), final fracture was initiated from a single internal micropore, located 0·5 to 1·1 mm below the specimen surface. Crack propagation from the micropore was in the Stage II mode and occurred about equally in all radial directions. This resulted in a circular crack with a relatively featureless surface (Fig. 1). When the crack pierced the specimen surface, it continued to propagate in the Stage II mode, but exhibited a rougher fracture surface (light regions just outside Stage II circle). The crack propagated in Stage II until the onset of tensile overload failure.

In specimens cycled at high total strain ranges ($0{\cdot}007 \leq \Delta\epsilon_T \leq 0{;}020$), there were a number of internal crack initiation sites at pre-cracked MC carbides and micropores. Crack propagation from these sites was in the Stage II mode, except for limited observations of small planar facets. The location of the initiation site for fracture at the highest strain ranges could not be determined because failure occurred somewhat prematurely at the base of the extensometer ridge

Considerable secondary cracking (cracks not associated with main fracture) originated at pre-cracked carbides and micropores at all strain ranges. Although most of the cracks were surface initiated, the cracks that led to failure at the low strain ranges started in the interior (Fig. 1). The few interior cracks that were observed were short and narrow (Fig. 2 (a)). In contrast, the average surface-initiated crack was much longer and wider (Fig. 2 (b)). Exposure of the surface-connected crack to the atmosphere during testing led to oxide formation in the crack and in the specimen area adjacent to the crack surface. A zone beneath the oxide was denuded of γ' precipitate (light etching region in Fig. 2 (b)). The oxide in the crack and the reduced constraint exerted on a crack at the surface were responsible for the increased width of surface-connected cracks. Some Stage II cracks showed crack branches inclined to the stress axis that appeared planar (arrows in Fig. 2 (b)).

The deformation at 1700 °F was homogeneous in that the dislocations were uniformly distributed and not confined to planar bands, as they are at lower temperatures (Fig. 3).

C. Crack initiation and propagation at 1400 °F (760 °C)

At the lowest strain ranges ($\Delta\epsilon_T = 0{\cdot}0048$ and one of two tests at $0{\cdot}0061$), cracks were initiated in the specimen interior at micropores or

MC carbides. The initial stage of propagation was on crystallographic facets, which were identified as {111} planes. Fig. 4 (a) shows a typical Stage I facet with an array of micropores at the initiation site (arrow). The features on these Stage I facets are similar to those previously found on Stage I facets formed at room temperature [10]. The steps on the facets make an angle of 60 degrees with respect to each other and are preferentially aligned in ⟨110⟩ directions. Therefore, they probably result from cracking on other {111} planes intersecting the facet. At these low strain ranges, almost all fatigue fracture was in the Stage I mode. Limited Stage II cracking occurred when a Stage I crack encountered a pre-cracked carbide oriented approximately normal to the stress axis. In such cases, the crack switched back to the Stage I mode when it was out of the stress field of the carbide.

At intermediate strain ranges ($\Delta\epsilon_T = 0{\cdot}0077$ and one of two tests at 0·0061), there were a few cracks initiated at interior pre-cracked MC carbides in each specimen and crack propagation was initially in the Stage II mode. The Stage II surfaces were relatively flat and featureless and crack propagation occurred radially. After the crack propagated a distance approximately equal to the carbide length, a sharp transition to Stage I occurred. These are believed to be the first observations in which Stage II cracking precedes Stage I. It was difficult to follow the sequence of cracking beyond this point because of link-up of separately initiated cracks.

At the highest strain ranges ($0{\cdot}0084 \leq \Delta\epsilon_T \leq 0;018$), the final fracture resulted from the link-up of a number of cracks initiated at the surface and in the interior. The surface-initiated cracks propagated initially in either the Stage I or II modes, but the interior-initiated cracks usually propagated initially in Stage II. A single crack often exhibited a number of Stage I and II segments (Fig. 5). The features on the Stage I facets (Fig. 4 (b)) consisted of equiaxed dimples (Fig. 4 (c)) and were similar to those on Stage I facets formed at room temperature at the same total strain range [7]. The Stage II fracture surfaces were relatively featureless (Fig. 6 (a)), except for limited regions containing striations (Fig. 6 (b)).

No secondary cracks were observed in specimens tested at the low and intermediate strain ranges. In the specimens tested at the highest strain ranges, there was some secondary cracking, most of it originating at the surface.

Much of the deformation at 1400 °F was similar to that at room temperature and occurred in coarse planar bands (Fig. 3). Compared to room temperature specimens, the dislocation density in the bands was reduced, and the many elongated dislocation loops were not associated solely with slip bands.

Discussion

A. The effect of temperature on crack propagation mode

At room temperature, most fatigue cracking is in the Stage I mode [7, 10]; whereas, at 1700 °F, it is in the Stage II mode. The temperature of 1400 °F represents a transition in which Stage I cracking occurs at low strain ranges and Stage II cracking occurs *initially* at the high strain ranges; later stages of cracking at the high strain ranges may be in either the Stage I or II modes. The transition in the mode of fatigue cracking with temperature can be related to the deformation behavior of this material.

At room temperature, all deformation is concentrated in coarse, planar bands (Fig. 3 (a)). Slip activity at low strain ranges is limited to, at most, a few parallel planes at the crack tip [7, 10]. Stage I cracks propagate on these planes and the features on the fracture surface, which are similar to those in Fig. 4 (a), resemble features found on cleavage fracture surfaces of bcc and hcp materials. At the higher strain ranges [7], complex deformation occurs within the slip bands and the bands are broadened. The Stage I fracture surface has a rougher appearance and contains a uniform distribution of equiaxed dimples, similar to those observed in Fig. 4 (c) and on ductile tensile fracture surfaces. In order to explain these unusual features on Stage I fracture surfaces, it has been proposed [7] that the slip activity lowers the cohesive energy of the band and, unlike cracking in the unslipping models [2, 6], the final separation occurs under the influence of the local normal stress at the crack tip. Alternatively, Stage I fractures may result from a local enhancement of the normal stress across the band, following the accumulation of particular dislocation arrays or defects in the bands.

At 1400 °F and low strain ranges, slip is confined to planar bands and the mechanism of Stage I failure is the same as that proposed for the room temperature case. Although deformation is mostly planar at the higher strain ranges as well, Stage II cracking occurs in the vicinity of carbides and micropores. The stress field around a micropore is more isotropic than that around a sharp fatigue crack [12]. This can lead to more homogeneous deformation around the micropore and, as a result, to the Stage II cracking that is observed. This effect will probably not be as large when the defect is a pre-cracked carbide. However, the thermally-generated dislocation tangles that are observed around carbides can locally induce more homogeneous deformation. Once the crack is out of the stress field of the defect, propagation is in the Stage I mode. Additional Stage II cracking can occur with increased crack length as the crack propagates into the vicinity of other defects. This occurs with greater frequency with increasing strain range because: (a) there is more secondary cracking (b) the stress fields around cracks and defects extend further and (c) slip may be more homogeneous [8].

At 1700 °F, most of the deformation is homogeneous and not confined to slip bands. This type of deformation, which is probably denser at the crack tip than in the typical field shown in Fig. 3 (c), leads to localized irreversible dislocation movements and Stage II cracking. The radial symmetry of the Stage II cracks (Fig. 1) is additional evidence for the homogeneity of the crack tip deformation.

Further possible confirmation of the effect of slip character (planar or homogeneous) on the mode of fracture was obtained in fatigue tests at 1400 °F at different strain rates [13]. It was found that the fraction of the fatigue area covered by Stage I facets increased with strain rate and there is evidence that this results from an accompanying increase in the planarity of slip. Additional work is planned in this area.

B. The influence of oxygen on crack initiation and the rate of crack propagation

A single crack from a single initiation site propagates to failure at low strain ranges at all temperatures. At room temperature, the initiation site is at the surface, and at 1400 °F and 1700 °F, it is in the interior. The final fracture at high strain ranges at all temperatures results from a link-up of a number of cracks originating both at and below the surface.

At room temperature and low strain ranges, cracks are initiated at the surface because of the greater stress concentration around surface-connected defects [14]. At the high strain ranges, cracks are initiated at less favorable sites as well, such as those in the specimen interior.

At 1700 °F, most cracks are surface-initiated, but at the low strain ranges, the crack that propagates to failure originates in the interior. The surface-connected cracks are filled with oxide, which extends right to the crack tip. The oxidation increases the crack tip radius (Fig. 2) and, by completely filling the area between the crack surfaces, reduces the amount of crack resharpening that is possible in the compressive-half cycle in the plastic blunting mechanism [5]. Both these effects serve to reduce the crack growth rate.* In contrast, the few interior-initiated cracks are small, narrow and unoxidized (Fig. 2). These results indicate the surface cracks are formed first, but that the cracks formed at a later time in the interior propagate more rapidly, and thus lead to failure.

At 1400 °F, similar results are obtained, except for the absence of microscopically observable surface cracks at the low and intermediate strain ranges. At this temperature, a thin, adherent oxide is formed which may have an effect on crack initiation as well as on propagation.

* It is not likely that the sintering of oxide in the cracks, which has been shown to increase creep and stress-rupture properties of nickel and nickel alloys [15, 16 , is effective because of the shorter sintering times and higher tensile stresses in the present tests.

Conclusions

1. All deformation at room temperature and most of that at 1400 °F (726 °C) is concentrated in coarse, planar bands. Either a reduction in cohesive energy of the slip band or a local enhancement of the normal stress across the band leads to Stage I cracking.
2. At 1700 °F (927 °C) and around microstructural defects at 1400 °F, the deformation is homogeneously distributed. The dislocation motion at the crack tip is irreversible and cracking is in the Stage II mode.
3. These results indicate that Stage I cracking is favored under conditions of planar slip and Stage II cracking under conditions of wavy or more homogeneous deformation.
4. At 1700 °F, surface-connected cracks are oxidized. As a consequence, the crack tip radius is increased and the amount of crack resharpening in the compressive-half cycle is reduced. Both these effects retard the growth rate of surface-connected cracks compared to those initiated in the interior and are responsible for the internal initiation of final failure at low strain ranges.

Acknowledgments

We would like to express our appreciation to G. M. Rowe for his assistance in electron microscopy and to Drs C. A. Rau, C. P. Sullivan and C. H. Wells for many helpful discussions.

References

1. FORSYTH, P. J. E. 'A two stage process of fatigue crack growth' *Proc. Crack Prop. Symp.*, College of Aeronautics, Cranfield, Beds, England, vol. 1, 1962, p. 76.
2. SHANLEY, F. R. *Colloquium on Fatigue*, IUATM, Springer-Verlag, Stockholm, 1955, p. 251.
3. AVERY, D. H. and BACKOFEN, W. A. *Fracture of Solids*, Interscience Publ., N.Y., 1963, p. 339.
4. FUJITA, F. E. *Fracture of Solids*, Interscience Publ., N.Y., 1963, p. 651.
5. LAIRD, C. *Fatigue Crack Propagation*, ASTM STP 415, Philadelphia, 1967, p. 131.
6. SCHIJVE, J. *Fatigue Crack Propagation*, ASTM STP 415, Philadelphia, 1967, p. 415.
7. GELL, M. and LEVERANT, G. R. *Trans. AIME*, in press.
8. WELLS, C. H. *Acta Met.*, in press.
9. McEVILY, A. J. and JOHNSTON, T. L. *Int. J. Frac. Mech.*, vol. 3, p. 45, 1967.
10. GELL, M. and LEVERANT, G. R. *Acta Met.*, vol. 16, 553, 1968.
11. WELLS, C. H. and SULLIVAN, C. P. *Trans. Quart. ASM*, vol. 57, p. 841, 1964.
12. RICE, J. R. *J. Appl. Mech.*, vol. 35, p. 379, 1968.
13. GELL, M. and LEVERANT, G. R. unpublished research.

14. TIMOSHENKO, S. and GOODIER, J. N. *Theory of Elasticity*, McGraw-Hill, New York, 1951, p. 82.
15. CASS, T. R. and ACHTER, M. R. *Trans. AIME*, vol. 224, p. 1115, 1962.
16. PRANATIS, A. L. and ACHTER, M. R. NRL Report 6516, March 6, 1967.

Fig. 1. An internally-initiated Stage II crack responsible for specimen failure at a low strain range at 1700°F, montage, 50×.

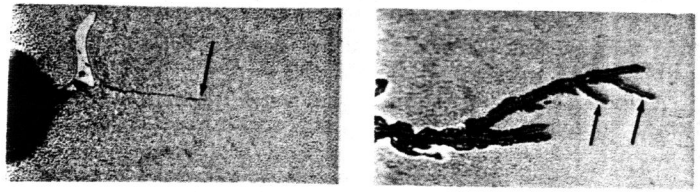

(a) (b)

Fig. 2. Secondary cracks in high-strain fatigue specimens at 1700°F (a) interior crack (arrow) initiated at MC carbide and micropore, (b) surface-initiated crack showing oxide and region denuded of γ' precipitate (light region) and possible crystallographic crack branching (arrows). Tensile axis is vertical. 550×.

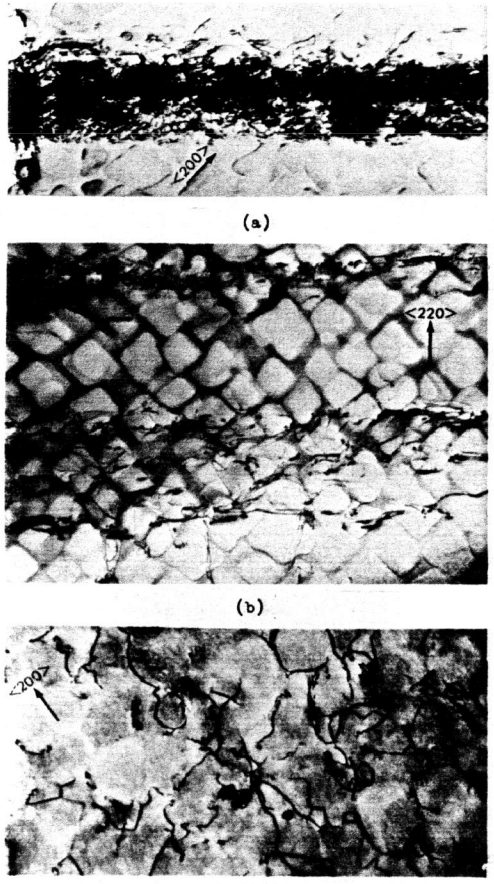

Fig. 3. Dislocation structures typical of specimens cycled to failure in the high strain region at (a) room temperature, (b) 1400°F, (c) 1700°F. 36,000 ×.

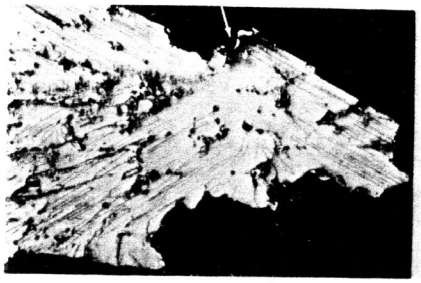

(a)

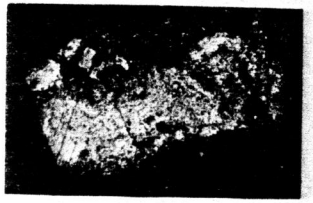

(b)

(c)

Fig. 4. Stage I facets on fracture surfaces of specimens cycled at 1400°F. (a) low strain range, 55×. (b) high strain range, 110×. (c) high strain range, 5000×.

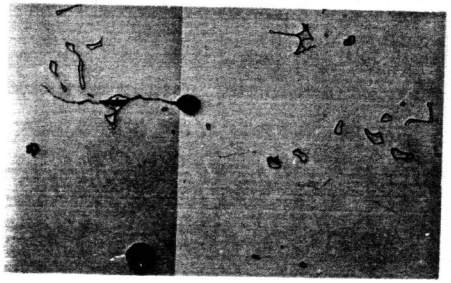

Fig. 5. An internally-initiated crack at a high strain range at 1400°F showing a number of Stage I and II segments, montage. Tensile axis is vertical. 220×

(a)

(b)

Fig. 6. Stage II facets on fracture surfaces of specimens cycled at 1400°F. (a) typical area with initiation site at MC carbide (arrow), 220×. (b) a region containing striations, 2500×.